Hindawi
International Journal of Aerospace Engineering
Volume 2022, Article ID 6439787, 12 pages
https://doi.org/10.1155/2022/6439787

Research Article

Thermal Decomposition, Ignition Process and Combustion Behavior of Nitrate Ester Plasticized Polyether Propellant at 0.1–3.0 MPa

Chengyin Tu,[1] Yaya Feng,[2] Zhigang Ling,[2] Xiong Chen,[1] Changsheng Zhou,[1] Yingkun Li,[1] Weixuan Li,[1] and Wenxiang Cai[1]

[1]*School of Mechanical Engineering, Nanjing University of Science and Technology, Nanjing 210094, China*
[2]*The Synthetic Chemical and Engineering Institute of Inner Mongolia, Hohhot 010010, China*

Correspondence should be addressed to Xiong Chen; chenxiongnjust@njust.edu.cn

Received 30 June 2022; Revised 26 September 2022; Accepted 10 October 2022; Published 18 November 2022

Academic Editor: Erkan Kayacan

Nitrate ester plasticized polyether (NEPE) propellant is widely used in solid rocket motors, having both good mechanical properties and high specific impulse. However, its ignition and combustion process are complex and need to be better understood. In this study, a high-pressure sealed combustion chamber was constructed, a thermogravimetry-differential scanning calorimetry was used to investigate the thermal decomposition process, and a high-speed camera was used to capture the ignition process and combustion behavior of the propellant. The results showed that the thermal decomposition process of this propellant could be divided into two stages. The first stage (50–350°C) was the major mass loss stage and exhibited typical features of BTTN, RDX, and AP decomposition. The second stage (350–500°C) was mainly accompanied by decomposition of the remaining components as well as slight oxidation of aluminum particles. The ignition process of NEPE propellant was divided into four stages, including the inert heating period stage, thermal decomposition stage, initial flame stage, and stable combustion stage. After the propellant absorbed heat, the propellant started to pyrolyze and gasify to generate flammable gas. When the temperature of the propellant surface reached the flammable gas ignition point, an initial flame was generated on the surface, which spread rapidly, covering the surface. The ignition delay time of the propellant was measured by a signal acquisition system, and a mathematical model was then established for the ignition delay time. The results showed that the ignition delay time decreased with increased laser heat flux and ambient pressure. Finally, the Vielle burning rate empirical formula was used to fit the burning rate data for the propellant. The resulting good fit was consistent with experimental measurements and showed that the formula was valid for predicting the NEPE propellant burning rate under 0.1–3.0 MPa nitrogen.

1. Introduction

Solid propellant, as the energy source for solid rocket motors, determines the energy characteristics of the rocket engine. Therefore, it is essential to improve the specific impulse of solid rocket motors [1]. Nitrate ester plasticized polyether (NEPE) is a significant breakthrough in the development of high-energy solid propellants, combining the advantages of composite propellants and double-base propellants with high-energy and good mechanical properties [2], while its standard theoretical specific impulse can reach 2685 N·s/kg [3]. In our previous investigation, uniaxial tensile tests have been conducted using a self-made confining-pressure system and material testing machine to study the influences of confining pressure and strain rate on the mechanical properties of NEPE propellant. Li et al. [4] have found that confining pressure and strain rate has a remarkable influence on the mechanical responses of NEPE propellant. As confining pressure increases (from 0 to 5.4 MPa), the maximum tensile stress and ultimate strain increase gradually. Then, Li et al. [5] have obtained stress-strain curves and mechanical properties of NEPE propellant under

varying confining-pressure conditions and strain rates. The results show that the compressive mechanical properties of NEPE propellant are remarkably influenced by the confining pressure and strain rate. The compressive strength under confining pressure is clearly larger than those without applied confining pressure. However, the thermal decomposition, ignition process, and combustion characteristics of NEPE propellant have not been studied.

The combustion of solid propellant is a comprehensive physical and chemical process including heat transfer, momentum transfer, mass transfer, and high-speed chemical reaction. Many scholars have studied the correlation between thermal decomposition and combustion from the perspective of heat transfer, mass transfer, transmission, and chemical reactions and deduced the relationship equation between the combustion rate and kinetic parameters of a chemical reaction. Zhou et al. [6] have investigated the influence of CL-20 on the thermal decomposition behavior of NEPE propellant by coupling differential scanning calorimetry, thermogravimetry, and infrared spectroscopy (DSC-TG-IR). Yuan et al. [7] have investigated the thermal decomposition of Al/AP/HTPB propellant, in which the propellant thermal decomposition process consisted of three stages.

There are several ways to ignite solid propellants, among which laser ignition has been widely used in recent years in ignition studies of solid propellants and metal particles. As an attractive heating source, a laser has high output energy and controllable loading time, which allows noninvasive, remote, and direct ignition of solid propellants. In the 20th century, Baer and Ryan [8], Hermance et al. [9, 10], Kashiwagi [11], Niioka et al. [12], and Kulkarni et al. [13] began research into the ignition performance of solid propellants, including ignition theory, test methods, and performance. Based on the earliest solid-phase ignition model, gas-phase ignition and heterogeneous ignition models have been established. In many ignition experiments, monopropellants [14], double-base propellants [15], and composite propellants [16] have been the main research objects. Sivan and Haas [17] have studied diode-laser ignition of pyrotechnic mixtures and investigated ignition delay time dependence on laser intensity, combustion temperature, and composition. Medvedev et al. [18, 19] have studied the dependence of the laser ignition energy threshold on sample density and dispersion using pulse laser and explained their results in terms of thermal ignition theory. Ehrhardt et al. [20] have studied the pyrolysis, ignition, and combustion of low-vulnerability propellants using lasers. The combustion characteristics they measured included ignition delay, maximal pressure, burning rate, and ignition energy. Compared with traditional composite propellants and double-base propellants, NEPE propellants contain numerous energetic components and have a narrow adjustable range of burning rate, and the adjustment technology of burning rate and pressure index are mutually restricted. However, the existing combustion models of composite propellants and double-based propellants cannot directly simulate the NEPE propellant combustion process, such that it is necessary to study the combustion characteristics of these propellants.

Research on laser ignition of NEPE propellant is relatively limited. Pang et al. [21] have investigated thermal decomposition behavior and nonisothermal decomposition reaction kinetics of a propellant containing ammonium dinitramide (ADN). Kong et al. [22] have used GGA/PBE and B3LYP methods in density functional theory to clarify the initial decomposition reaction of ammonium perchlorate (AP) and the oxidative cross-linking reaction mechanism in propellants. Zhu et al. [23] have examined the effects of laser heat flux density on the ignition delay time of propellants. Wang et al. [24] have analyzed the influence of laser heat flux on the ignition delay time of propellants and found that the ignition delay time has an exponential relationship with the laser heat flux. Xiang et al. [25] have studied the influence of oxygen content in the environment gas on the first flame position and ignition delay time of propellants. Yan et al. [3] have measured the burning rate and burning surface temperature of four new NEPE propellants, observed their combustion flames, analyzed the effects of different propellant components on the burning rate, and improved the radical cracking model such that it can be used to predict the burning rate of these propellants. Li et al. [26] have used a high speed camera and IR thermometer to investigate the ignition, combustion, and surface temperature distribution of propellants under laser irradiation and then established the ignition mechanism and combustion dynamics model of the propellant. Tu et al. [27] have studied the combustion characteristics of NEPE propellant in nitrogen (N_2) and air and found that the burning rate of NEPE propellant is greatly affected by the environment gas. Meanwhile, they have observed the agglomeration of aluminum (Al) particles on the combustion surface of NEPE propellant and studied the agglomeration process [28], agglomeration mechanism [29], and movement behavior of aluminum particles [30].

The previous study here mainly focused on quantitative research on the laser ignition of NEPE propellants, while little attention was paid to variations of the propellant surface during the ignition process. In this study, a TG analytical model was used to study the thermal reaction process of NEPE propellant and examine the influence of different laser heat fluxes and ambient pressure on the ignition process as well as combustion characteristics of the propellant studied using a laser ignition test platform. The experimental data were then associated with a theoretical analytical model to analyze the behaviors of ignition and combustion. The results were helpful for further understanding the thermal decomposition, ignition process, and combustion behavior of NEPE propellant.

2. Experimental Setup

2.1. Materials. The main components of NEPE propellant used in these experiments included a cross-linking agent (polyethylene glycol, CAB, 6–8%, 20–30 μm), plasticizer (nitroglycerine/1,2,4-butanetriol trinitrate, BTTN, 17–21%), AP particles (20%-30%, 100–150 μm), Al particles (20–30%, 3–7 μm), RDX particles (18–20%, 20–30 μm), curing agent (polyvinyl chloride, PVC, 1–2%), and catalyst (chromic oxide, Cr_2O_3 and carbon black, CB, 1–2%). In an

experiment, the specimen dimensions were $5 \times 5 \times 5$ mm. To ensure accuracy of the experimental data and clarity of experimental phenomena, high temperature resistant insulating rubber was coated around the experimental sample to prevent sample side-burning before the experiment.

The material used in this investigation was a NEPE propellant and the composition listed in Table 1. A scanning-electron-microscopy (SEM) image of the NEPE propellant showed large particles that were AP and the main portion the plasticizer, with Al, RDX, and other constituents distributed randomly inside the matrix (Figure 1).

The propellant was prepared according to the following steps: first, mixed solid materials were added to the prepared liquid material, and then all materials were mixed in a vertical kneader for 1 h. Second, the obtained propellant slurry was degassed and cured in a vacuum oven at 50°C for 7 d. At last, the resulting solid propellant was cut into samples of the required size to meet experimental needs.

2.2. Experimental Apparatus. A TGA/SDTA851E thermal gravimetric analyzer and DSC823E differential scanning calorimeter (Mettler-Toledo International Inc., Greifensee, Switzerland) were used to investigate the thermal decomposition behavior of propellant samples. Tests were performed under N_2 at atmospheric pressure. Approximately 0.5 mg of sample was placed in an Al_2O_3 crucible and heated from 50 to 550°C at a rate of 10°C/min.

Experiments were carried out on a sealed high-temperature and high-pressure laser ignition platform. The experimental system was mainly composed of a control system, CO_2 laser optical system, combustion chamber, and data acquisition system (Figure 2, schematic diagram). The control system was composed of computer software and a control card, which was used to adjust the laser loading time and heat flux density of the CO_2 laser. The CO_2 laser had a power of 300 W and wavelength of 10.6 μm. The optical system changed the horizontal laser beam emitted by the laser into a vertical laser beam and applied the beam to the surface of the test piece through a l20 mm diameter laser entrance window on the combustion chamber top. The optical system consisted of a plane mirror and a focusing mirror at the top of the combustion chamber, which was $150 \times 150 \times 300$ mm. The maximum working pressure of the chamber was 4 MPa and there was a 50×100 mm observation window in the horizontal direction. The data acquisition system used two photodiodes to collect the laser light signal and propellant initial flame signal to obtain the propellant ignition delay time. When the laser light started to emit light, the photodiode collected the signal and converted it into an electrical signal. The amplified electrical signal was output to the LED, which then emitted light that was captured by the high-speed camera and regarded as the starting point of the laser ignition process. In addition, the experimental system was also connected with high speed cameras to monitor the combustion process in the combustion chamber. The ignition and combustion processes were recorded by a high speed camera (Chronos 1.4, Kron Technologies Inc., Burnaby, Canada) at a frame rate of 1000 fps, with the camera aperture in experiments at the smallest aperture to ensure that the propellant did not create overexposure during burning.

2.3. Experimental Methods. A summary of all experimental conditions is shown in Table 2. Multiple test repetitions under each experimental condition were performed to ensure test data reliability. The pressure in the combustion chamber was adjusted using high-pressure cylinders, and the ambient pressure in the chamber was detected by a pressure sensor to meet experimental requirements. The signal acquisition system was triggered synchronously with the laser loading system to measure the ignition delay time. When the NEPE propellant was ignited by the laser and the flame spread to the entire sample surface, it was recorded as the beginning of propellant combustion. When the propellant flame height drops to half of the stable combustion flame height, propellant combustion was considered to be ending. The burning rate was calculated from the burning process captured by high speed camera [31, 32].

3. Results and Discussion

3.1. Thermal Decomposition Characteristics Analysis. The TG-DTG and DSC curves for the propellant showed that the overall trend of the TG curve indicated a two-stage thermal decomposition at 50–550°C (Figure 3). Propellant samples underwent different reaction processes in each stage, resulting in multiple endothermic and exothermic peaks on DSC curves.

Stage (I) was a fast-mass-loss stage from 50 to ~350°C, accompanied by a 70% mass loss. Examining the TG curve in this temperature range, three substages were further distinguished, with ranges of 100–200, 200–250, and 250–350°C. First, at 100–200°C, mass loss was ~15%, with the first DTG peak around 148.3°C. The first exothermic peak appeared at 185.7°C, which might have been caused by decomposition of plasticizer BTTN, as for pure BTTN, the decomposition temperature is 230°C [33], while AP and RDX in the propellant promoted BTTN decomposition.

Second, at 200–250°C, the process was mainly the decomposition of RDX, CAB, and the remaining BTTN, with a mass loss of ~45%. The second DTG peak appeared at 243.3°C and second exothermic peak at 218.3°C. In a previous study, the DSC peak of the exothermic decomposition of pure RDX was at 240.1°C [34], with the DSC peak of RDX exothermic decomposition dropping to 218.3°C caused by AP [35]. The accelerating effect of AP on the RDX decomposition peak and lowering of the RDX melting point, resulting in accelerated decomposition and initial AP dissociation which produced strong oxidizing gas-phase products might be the main factors in this process.

Finally, at 250–350°C, the process was mainly AP decomposition, with a mass loss of ~10%. AP, as an oxidant, is commonly used in NEPE propellant, with its thermal decomposition having a great influence on the combustion process. AP thermal decomposition was divided into two stages: low and high temperature, with different decomposition mechanisms. The endothermic peak at 249.2°C represented the crystalline phase transition process of AP from

Table 1: Composition of NEPE propellant.

Component	Content (wt%)	Particle diameter (μm)
AP (ammonium perchlorate)	20–30	100–150
Al (aluminum)	20–30	3–7
BTTN (nitroglycerine/1,2,4-butanetriol trinitrate)	17–21	
CAB (polyethylene glycol)	6–8	
RDX	18–20	20–30
PVC (polyvinyl chloride)	1–2	
Catalyst	1–2	

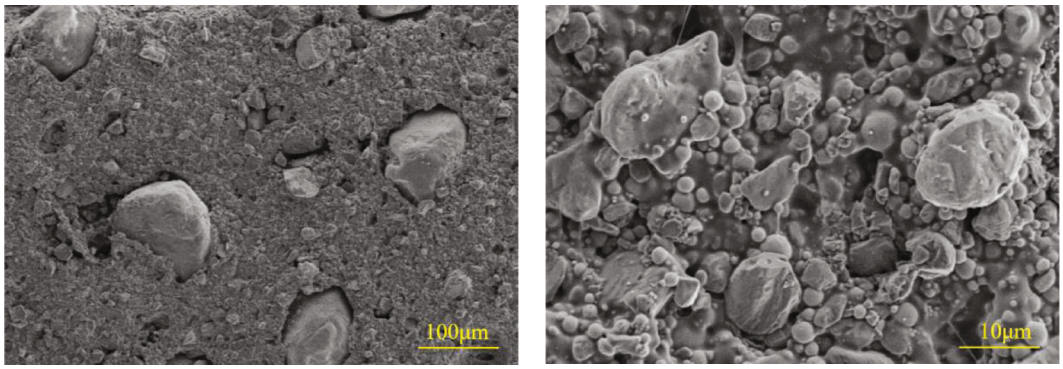

(a) (b)

Figure 1: SEM image of the propellant surface.

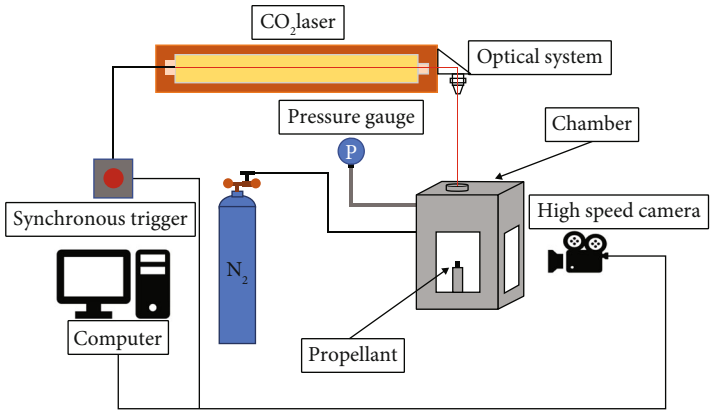

Figure 2: Schematic of the experimental system.

Table 2: List of test conditions.

Test conditions	Values
Pressure (MPa)	0.1, 0.5, 1.0, 1.5, 2.0, 2.5, 3.0
External heat flux (W/mm^2)	1.00, 1.75, 2.50
Inlet air temperature (°C)	25
Gas atmosphere	N_2

an orthorhombic to cubic form, during which no mass loss occurred [36]. This endothermic peak was in good agreement with previous reports [36, 37]. The second stage of AP decomposition corresponded to the third exothermic peak (301.2°C) in the DSC curve, during which AP weight loss reached 50% [38]. AP decomposition produced a variety of oxidizing gases, which released further heat and accelerated thermal decomposition of AP and RDX.

Stage (II) was a high-temperature slow heat release stage (350–550°C). During this process, the sample mass changed slightly and there were no exothermic and endothermic peaks in the DSC curve. When the temperature was >350°C, only Al particles and decomposition products of residual components were left. As the temperature continued to increase, the sample mass slowly decreased, releasing a small amount of heat, and when the temperature reached

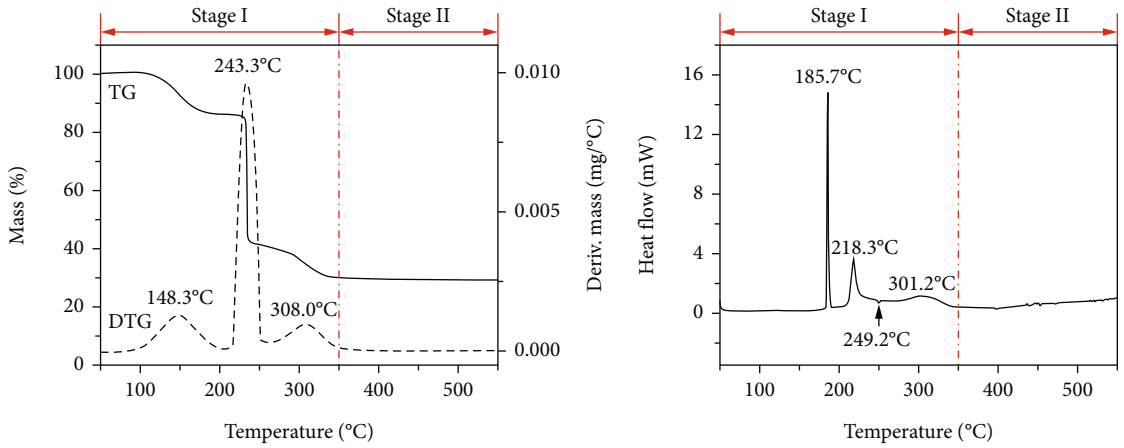

(a) Curves of TG-DTG for NEPE propellant

(b) Curves of DSC for NEPE propellant

Figure 3: TG-DTG and DSC curves for NEPE propellant.

550°C, the mass of remaining material was 29.3% of the initial mass.

3.2. Ignition Process. The ignition process of the solid propellant involved a series of intricate physical and chemical processes. The ignition combustion process of NEPE propellant under 1.5 MPa N_2 and a heat flux of 1.75 W/mm^2 is shown in Figure 4. Based on previous research, the ignition process of this propellant can be divided into four stages: the inert heating period, thermal decomposition, initial flame, and stable combustion [26]. When $t = 0$ s, laser radiation was emitted to the propellant specimen surface and the solid phase temperature rose with increased absorbed radiant energy. At $t = 0.300$ s, there was no significant change in the propellant surface and thus called the inert heating period. In the next stage, when the temperature of the solid phase reached the melting point, the solid phase component began to melt to form a paste-like area composed of solid and liquid phases on the specimen surface. As the propellant surface continued to absorb heat, a portion of the liquid phase underwent pyrolytic reactions and yielded gas products. At the same time, the gas phase products quickly evaporated from the propellant surface and entered the surrounding ambient gas to form a pyrolytic gas. When $t = 0.312$ s, white smoke began to appear on the propellant surface, which meant that the propellant had begun to gasify. The resulting flammable gas evaporated off the surface and the pyrolytic gas reacted or decomposed to form other gaseous substances. These substances could oxidize and release a large amount of heat in the gas phase. This stage was called the thermal decomposition period.

When the temperature of the propellant surface reached the ignition point of the pyrolytic gas, the propellant surface produced an initial flame (Figure 4(c)) called the initial flame period. Then, the initial flame spread rapidly on the propellant surface, gradually covering the entire surface as the flame intensity increased. At this time, thermal feedback from the gas-phase exothermic reaction maintained the solid-phase exothermic reaction such that the propellant achieved a stable combustion stage (Figures 4(d) and 4(e)). When $t = 1.108$ s, laser irradiation was interrupted and the propellant maintained a stable combustion. This was because the decomposition heat of propulsion and flame feedback heat maintained stable propellant combustion.

During the ignition process of the NEPE propellant, the condensed phase was transformed into a gaseous phase. On one hand, it was through physical evaporation and sublimation, but on the other hand, the main form was that propellant components became gaseous products through pyrolysis on the combustion surface. Therefore, it was generally believed that pyrolysis was the initial stage of the propellant ignition process. The gaseous products of pyrolysis then underwent further combustion reactions. The combustion process of solid propellant is usually divided into two major areas: condensed and gas phase reactions. The condensed phase reaction is mainly composed of pyrolytic reactions of the oxidant and binder in the propellant and reactions between decomposition products. The product of the condensed phase reaction or substances produced by condensed phase gasification enters the gas phase and further undergoes combustion reactions. Although the actual combustion reaction of the propellant occurred in the gas phase, as gas phase reactions were much faster than condensed phase reactions, the importance of condensed phase reactions in the combustion process of the propellant was realized.

3.3. Ignition Delay Time

3.3.1. Analytical Model of Ignition Delay Time. Ignition characteristics are important performance parameters of the solid propellant. On one hand, the ignition performance of the solid propellant is an important basis for the analysis of the ignition process of the solid rocket motor and the igniter design. On the other hand, research on the ignition performance of solid propellant has also played an essential role in guiding the development of propellant formulations. The ignition delay of the solid propellant refers to the time from when the laser starts to load energy to the propellant until the propellant is ignited. According to literature [26],

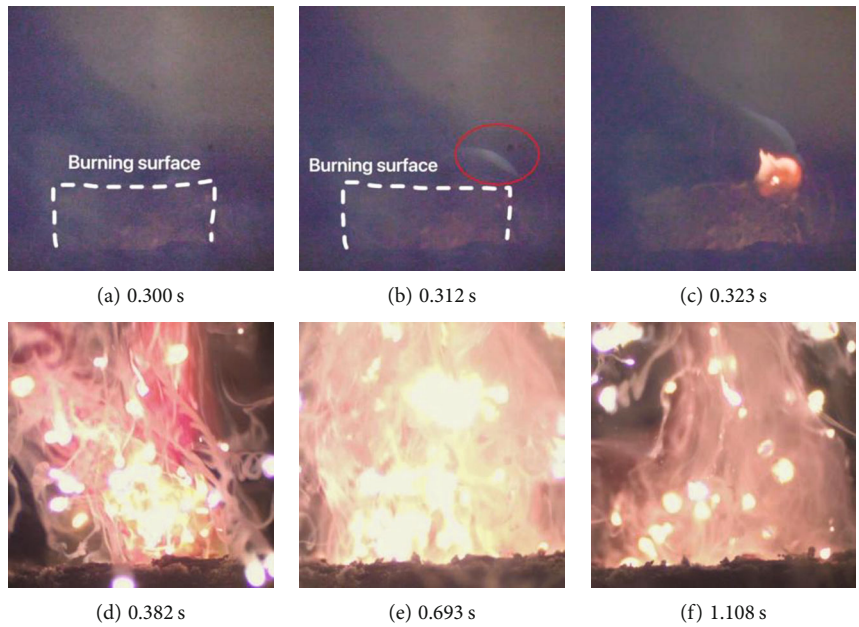

(a) 0.300 s (b) 0.312 s (c) 0.323 s

(d) 0.382 s (e) 0.693 s (f) 1.108 s

Figure 4: Ignition process of NEPE propellant.

the ignition delay time t_{ig} consists of two parts: the pyrolysis time (t_{py}) and gas phase chemical reaction time (t_{chem}).

$$t_{ig} = t_{py} + t_{chem}. \tag{1}$$

The ignition process of NEPE propellant is quite complicated and only after detailed analysis can the exact value of t_{ig} be obtained. Two characteristic times that affect ignition delay represent the two main processes leading to this delay. First, the laser is irradiated on the propellant surface, and the propellant is rapidly heated to a high enough temperature to thermally decompose to produce pyrolytic products containing gaseous fuel. The period until the output of pyrolytic products reaches the minimum value required for propellant combustion is called t_{py}. Once the flammable mixture gains enough energy, there is another moment in time for the chemical reaction to proceed to "thermal runaway" or a flaming condition. This step involves the time needed for the flammable mixture to proceed to combustion, which is called t_{chem}.

According to the previous research [39],

$$t_{py} = \frac{\pi \rho_s C_p k \left(T_{py} - T_\infty\right)^2}{4 q_0^2}, \tag{2}$$

where ρ_s is the solid density, C_p the special heat, k the thermal conductivity, T_{py} the pyrolytic temperature, T_∞ the ambient temperature, and q_0 is the laser heat flux density.Therefore, $\pi \rho_s C_p k (T_{py} - T_\infty)^2/4$ can be regarded as a constant, called the thermal response parameter, which is one of the material properties that combine ignition temperature with density, specific heat, and material conductivity. Therefore, t_{py} is inversely proportional to the quadratic power of the laser heat flux density, expressed as

$$t_{py} \propto \frac{1}{q_0^2}. \tag{3}$$

The mathematical formula of the chemical reaction time was expressed as [26]

$$t_{chem} = \frac{CkT_\infty}{\alpha [E/(RT_\infty)] \Delta h_c A e^{-E/(RT_\infty)}}, \tag{4}$$

where C is the constant coefficient, k the thermal conductivity, T_∞ the ambient temperature, α the thermal diffusivity coefficient of the gas mixture, E the activation energy, R the gas constant, Δh_c the heat of combustion, and A is a pre-exponential factor.

According to the heat transfer and chemical kinetics laws, t_{chem} is inversely proportional to the quadratic power of the pressure [40], expressed as

$$t_{chem} \propto \frac{1}{p^2}. \tag{5}$$

The chemical reaction delay was quite small and ignored here. Therefore, it was difficult to obtain an accurate t_{chem} value through experiments and theoretical calculations and only the factors that affect it could be analyzed. This analysis indicated that t_{ig} could be calculated using Eq. (2) and Eq. (4). In practice, it was difficult to obtain the exact value of the gas-phase chemical reaction time t_{chem}. Therefore, most solid propellant ignition analytical models assume that the delayed ignition time t_{ig} is equal to pyrolysis time t_{py} [41, 42]. In this study, two characteristic time theoretical models were established to estimate the expected value based on relevant parameters, and the factors that affected the actual

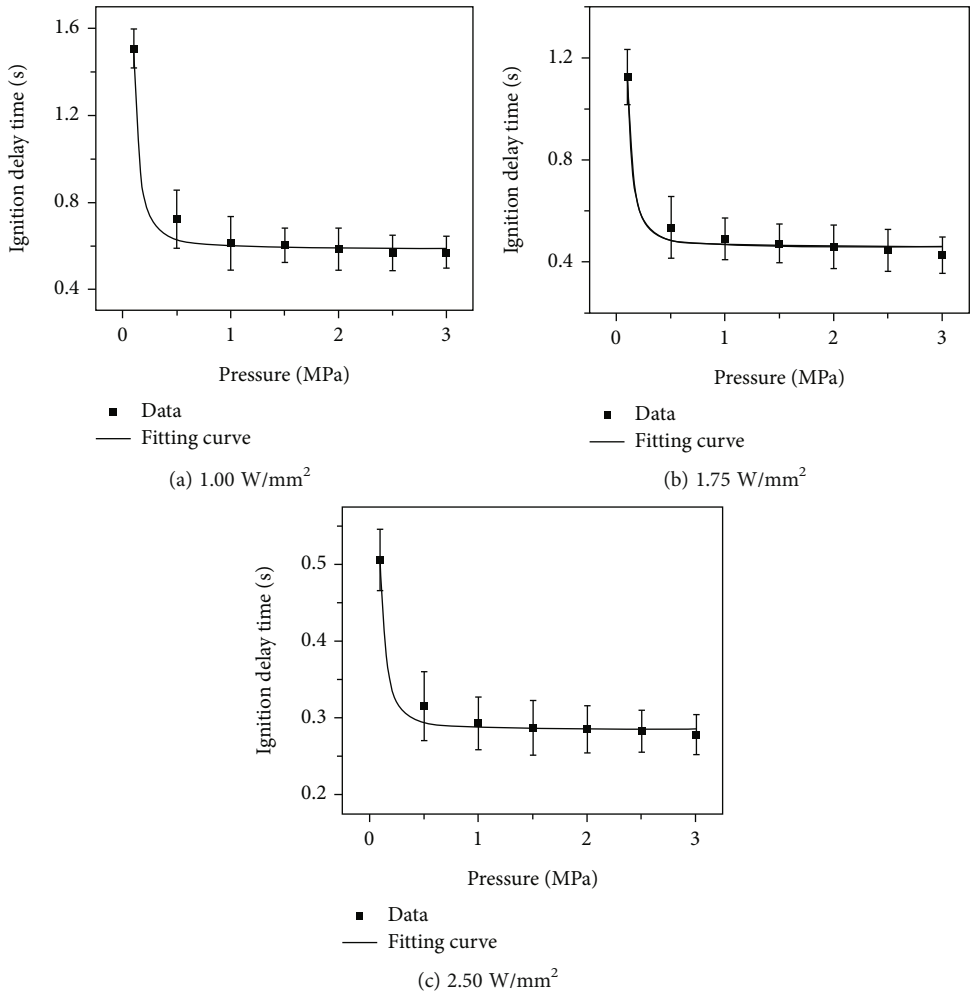

Figure 5: Curves of ignition delay time vs. pressure.

ignition process of most solid propellants were qualitatively analyzed. The relevant parameters, such as k, C_p, and ρ, could not be expected to be equal to the values found in the literature for common generic materials as temperature variations in the least will make them change. Although these effects were not considered in the modeling, the effective properties were still used to explain the ignition behavior.

3.3.2. Influence of Pressure on Ignition Delay. To understand the individual effect of pressure on the ignition delay time, laser ignition experiments were carried out under 1.00, 1.75, and 2.50 W/mm^2 and the ignition delay time of NEPE propellant was measured under 0.1, 0.5, 1.0, 1.5, 2.0, 2.5, and 3.0 MPa. To ensure experimental data accuracy, quintuplet experiments were carried out under each set of working conditions and the results averaged (Figure 5). The ignition delay time was seen to decrease as pressure increased. When the laser heat flux was 1.00 W/mm^2, as the pressure increased from 0.1 to 3.0 MPa, the ignition delay time was reduced from 1.5 to 0.6 s. When the laser heat flux was 1.75 W/mm^2, as the pressure increased from 0.1 to 3.0 MPa, the ignition delay time was reduced from 1.1 to 0.42 s. As the heat flux increased to 2.50 W/mm^2, the ignition delay time was reduced from 0.5 to 0.3 s. This effect was because a decrease in pressure increased the diffusion rate of pyrolytic products into the surrounding environment and reduced the collision frequency of molecules and the rate of chemical reactions, such that the chemical reaction area was far away from the propellant surface. At the same time, when the exothermic reaction zone moved away from the propellant surface, thermal feedback available to the propellant surface decreased, resulting in a longer ignition delay

Table 3: Fitting results of ignition delay time under different pressures.

Heat flux, W/mm^2	Fitting parameters	Correlation coefficient, R^2
1.00	$a_1 = 0.00920$, $b_1 = 0.58872$	0.99208
1.75	$a_2 = 0.00668$, $b_2 = 0.45880$	0.98441
2.50	$a_3 = 0.00221$, $b_3 = 0.28329$	0.97811

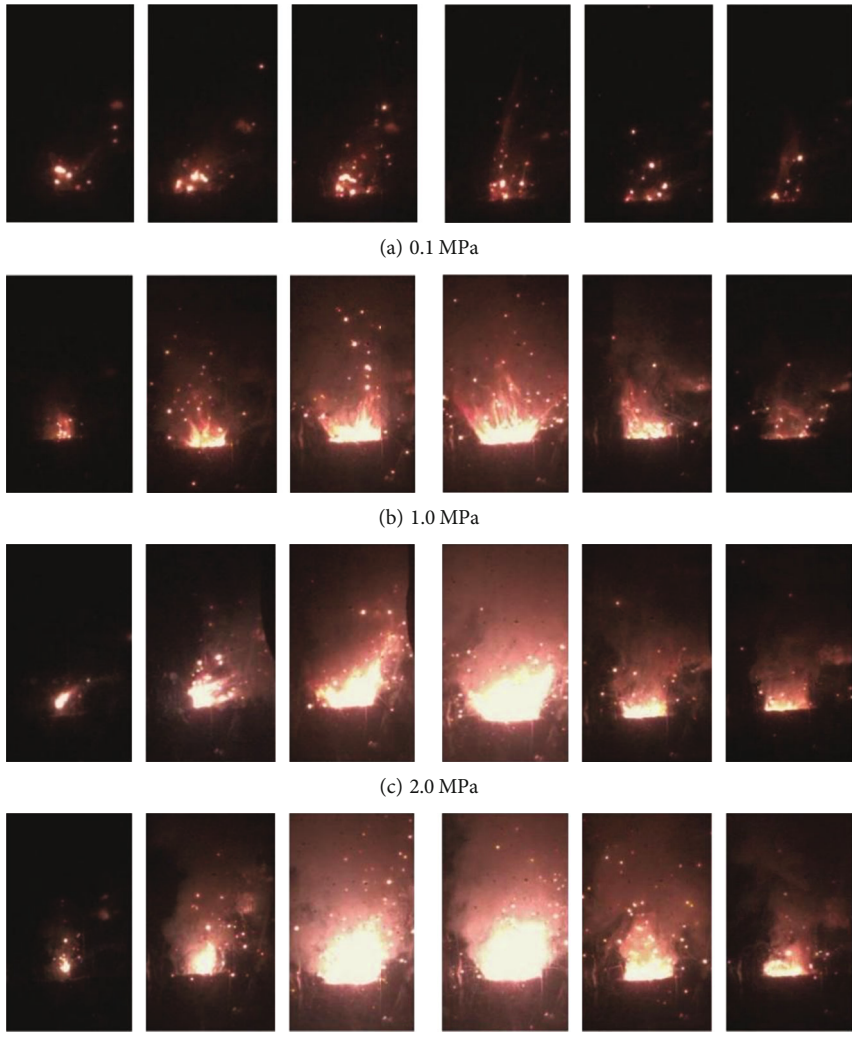

(a) 0.1 MPa

(b) 1.0 MPa

(c) 2.0 MPa

(d) 3.0 MPa

Figure 6: Combustion process of NEPE propellant.

time. When the pressure increased, the situation was reversed. For most solid propellants, there is a critical pressure value. When the pressure increases to this critical value, the influence of pressure on the ignition delay time can be ignored. In this experiment, when the pressure exceeded 1.0 MPa, the ignition delay time of the solid propellant was independent of the pressure.

At the same time, increasing the laser heat flux also reduced the ignition delay time of the propellant. In particular, in a normal pressure environment, the ignition delay time was significantly reduced. When p was 0.1 MPa, the heat flux increased from 1.00 to 2.50 W/mm^2 and the ignition delay time reduced from 1.5 to 0.5 s. However, when p was 3.0 MPa, the influence of heat flux was diminished and the ignition delay time decreased from 0.6 to 0.3 s, with the reduction significantly smaller than in the normal pressure environment. This was because increasing the heat flux sped the decomposition rate of the propellant, and in a high-pressure environment, decomposed gas accumulated on the propellant surface did not diffuse before reaching the minimum value required for ignition. Therefore, in a high pressure environment, the influence of heat flux was reduced.

According to the theoretical analysis of ignition delay time, t_{chem} was inversely proportional to the square of the pressure, which was combined with the mathematical model of pressure and ignition delay time established by Zarzecki et al. [43]. The above mathematical model was developed to make it more consistent with the NEPE propellant ignition characteristics. In these experiments, when the laser heat flux was constant, the relationship between ignition delay time t_{ig} and pressure was expressed as

$$t_{ig} = \frac{a}{p^2} + b, \tag{6}$$

where t_{ig} is the ignition delay time (s), p is the pressure of the combustion chamber (MPa), and a and b are the fitting parameters. The least square method was employed to fit the average of the five measurement results under each working condition. The fitting curves under different laser

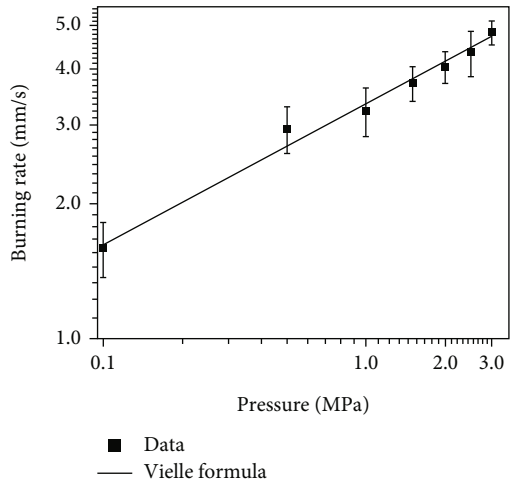

FIGURE 7: Burning rate fitting curve of NEPE propellant in N_2.

heat flux densities are shown in Figure 4, and the fitting results are listed in Table 3. For different laser heat flux densities, the fitting parameters of ignition delay time to ambient pressure were different, the reason for which might have been that with decreased heat flux, the influence of pressure on the ignition delay time became increasingly greater.

3.4. Combustion Process. In experiments, the ambient pressure had a significant effect on the combustion process of NEPE propellant. Under 1.75 W/mm^2 of heat flux, laser ignition experiments were performed under different ambient pressures to study the effects of pressure on the combustion behavior of NEPE propellant. The combustion process of NEPE propellant under different pressures was captured by a high speed camera (Figure 6).

Observations of the combustion process of NEPE propellant under 0.1, 1.0, 2.0, and 3.0 MPa showed that in the early stage of ignition formation, the propellant absorbed laser energy and decomposed into heated pyrolytic gas (Figure 5). The pyrolytic gas diffused above and around the surface of the propellant while metal particles on the surface absorbed the laser energy and produced sparks. The initial flame shapes formed under four different environmental pressures were not the same. When p was 0.1 MPa, only bright spots were observed on the propellant surface; when p was 1.0 MPa, only weak flames were generated on the surface; when p was 2.0 and 3.0 MPa, an initial spherical flame formed on the surface.

When p was 0.1 MPa, no apparent flame was observed to be formed during the entire process of loading the laser, but there was continuous burning. When the pressure was higher than 1.0 MPa, the flame shape was clearly observed. When the pressure was lower, the flame shape showed a clearer spreading shape. The propellant flame under 3.0 MPa environmental pressure was the most strong and bright. During the combustion process, a large amount of white smoke filled the entire combustion chamber and Al particles splashed out from the propellant surface. Under 1.0 and 2.0 MPa, the flame was darker and the upper flame parts swung violently, which indicated more turbulence. The reason for this phenomenon might have been because when the pressure was high, the pyrolytic gas generated by propellant surface thermal decomposition lingered on the surface and the corresponding oxygen content was higher, which made combustion more complete, the flame brighter and stronger, and thus the pressure higher. When the pressure was low, the pyrolytic gas diffused rapidly and the gas fuel and oxygen content on the surface was relatively low, making the flame darker, which easily caused flame turbulence.

3.5. Burning Rate. The burning rate refers to the mass loss rate of the condensed phase fuel, which can be approximately expressed by the retreat distance of the combustion surface per unit time. To verify the effect of ambient pressure on the burning rate of NEPE propellant, the burning rate was measured under 0.1–3.0 MPa. High-speed imaging is a dynamic measurement method for measuring propellant combustion by recording the combustion process of solid propellant. According to the playback of sequence images of the propellant combustion process captured by high-speed camera, the burning rate of NEPE was calculated (Figure 7).

The formula commonly used to characterize the combustion of propellant is Vielle's law [6, 44].

The Vielle burning rate formula is

$$\dot{r} = a_v \cdot p^n, \tag{7}$$

where $\dot{r}$ is the burning rate (mm/s), p the ambient pressure (MPa), a_v the burning rate coefficient of Vielle's law, and n the burning rate pressure index.

To verify the comprehensive influence of ambient pressure on the burning rate of NEPE propellant, in the present laser ignition combustion experiment system, the burning time of the propellant was obtained using the diode signal of the test system, in which the burning rate at various pressures was obtained by calculation. To ensure test data accuracy, a number of repetitive tests were performed under each test condition, using the Vielle formula to perform regression analysis on the average burning rates under different ambient pressures.

When the ambient pressure increased from 0.1 to 3.0 MPa, the burning rate increased from 1.5 to 5.0 mm/s, which showed that higher pressure significantly promoted propellant combustion. The propellant surface absorbed laser heat and began to decompose, with the decomposed gases diffusing, mixing, and burning in the gas phase, which provided complicated environmental gas, temperature, and pressure conditions for propellant ignition and combustion. When the pressure increased, the thermal decomposition of RDX, CAB, BTTN, and AP in the NEPE propellant was more intense, resulting in a higher oxygen concentration near the combustion surface, thereby improving overall combustion intensity [45, 46]. Meanwhile, a carbon frame (deposit char layer) was formed on the burning surface, and catalyst particles accumulated on this skeleton without clumping. In a high pressure environment, the exothermic

reaction of the catalyst was more intense, which further increased propellant burning rate [47].

The burning rate measurements were fitted by a power function (Figure 7), expressed as

$$\dot{r} = 3.34 \cdot p^{0.31}, \quad (8)$$

where the correlation coefficient $R^2 = 0.9881$.

According to the regression curve and regression coefficient, the Vielle burning rate formula was seen to be in good agreement with the experimental results ranging from 0.1 to 3.0 MPa. Therefore, the Vielle burning rate formula was used to predict the burning rate of NEPE propellant in 0.1–3.0 MPa of N_2.

4. Conclusions

This study investigated the thermal decomposition, ignition, and combustion characteristics of NEPE propellant, and the results were analyzed and discussed in the following:

(1) According to TG-DTG and DSC curves, the thermal decomposition process of the propellant was divided into stages: the first stage (50–350°C) was a major mass loss stage, with 70% mass loss, because of the decomposition of BTTN, AP, and RDX. The second stage (350–550°C) was a high-temperature slow heat release stage, with slight mass changes, and there was no exothermic and endothermic peaks in the DSC curve

(2) The ignition process of NEPE propellant was divided into four stages. The first stage was the inert heating period of the propellant surface. In the second stage, the propellant surface temperature increased, the propellant began to pyrolyze, and the resulting combustible gas evaporated and diffused into the surrounding gas phase. The third stage was from the first vaporization to the first flame moment. At this stage, gas produced by pyrolysis was mixed with ambient gas. When the temperature reached a sufficiently high temperature, pyrolytic gas and oxidizing gas in the air started to burn and react and an initial flame appeared. The fourth stage was the process in which the propellant was completely ignited. The initial gas phase flame quickly moved to the surface of the propellant and finally ignited the propellant to achieve stable combustion

(3) Theoretical analysis on ignition delay time was performed, and NEPE propellant experiments were conducted under different laser heat fluxes and ambient pressures. The influence of laser heat flux and ambient pressure on propellant ignition delay time was analyzed and the ignition delay time mathematical model was verified. With increased environmental pressure and laser heat flux, the ignition delay time decreased, but the degree of influence was different, with the influence of laser heat flux greater

(4) NEPE propellant ignition experiments were carried out under N_2 at different pressures. The results showed that the combustion process of the NEPE propellant varied. As N_2 pressure increased, combustion became more intense. When the propellant was ignited under normal pressure, no clear flame was formed on the propellant surface. When p was 1.0 MPa, the propellant produced a weak flame, but when p was 2.0 or 3.0 MPa, the burn was violent and emitted bright light, accompanied by dense white smoke

(5) The burning rate of NEPE propellant increased with increased ambient pressure, because higher pressure promoted thermal decomposition of RDX, CAB, BTTN, and AP as well as the catalyst exothermic reaction. At the same time, increased propellant decomposition products added to combustion led to higher flame brightness. The Vielle burning rate formula was used to fit the burning rate of the NEPE propellant in 0.1–3.0 MPa N_2, and the fitting results were very consistent, such that the Vielle burning rate formula was used to predict the burning rate of NEPE propellant in 0.1–3.0 MPa of N_2

Data Availability

The data used to support the findings of this study are included within the article.

Conflicts of Interest

The authors declare that they have no conflict of interest.

Acknowledgments

This research was supported by the National Natural Science Foundation of China (No. 52006099), the Fundamental Research Funds of the Central Universities (Nos. 30920021102 and 309181B8812), and the Six Talent Peaks Project of Jiangsu Province of China (No. 2016-HKHT-017).

References

[1] X. Liu, W. Ao, H. Liu, and P. Liu, "Aluminum agglomeration on burning surface of NEPE propellants at 3-5 MPa," *Propellants Explosives Pyrotechnics*, vol. 42, no. 3, pp. 260–268, 2017.

[2] Y. J. Luo and J. R. Liu, "Research progress of high energy solid propellant," *Chinese Journal of Energetic Materials*, vol. 15, no. 4, pp. 407–410, 2007.

[3] X. T. Yan, Z. X. Xia, L. Y. Huang et al., "Study on the ignition process and characteristics of the nitrate ester plasticized polyether propellant," *International Journal of Aerospace Engineering*, vol. 2020, no. 4, Article ID 8858057, p. 10, 2020.

[4] H. Li, J. S. Xu, J. M. Liu, T. Y. Wang, X. Chen, and H. W. Li, "Research on the influences of confining pressure and strain rate on NEPE propellant: experimental assessment and constitutive model," *Defence Technology*, vol. 17, no. 5, pp. 1764–1774, 2021.

[5] H. Li, J. S. Xu, X. Chen et al., "Experimental investigation and modeling the compressive behavior of NEPE propellant under confining pressure," *Propellants, Explosives, Pyrotechnics*, vol. 46, no. 7, pp. 1023–1035, 2021.

[6] S. P. Zhou, F. Wu, G. Tang et al., "Influence of CL-20 content and particle size gradation on combustion performance of NEPE propellant," *Chinese Journal of explosives & propellants*, vol. 43, no. 2, pp. 195–202, 2020.

[7] J. Yuan, J. Liu, Y. Zhou, Y. Zhang, and K. Cen, "Thermal decomposition and combustion characteristics of Al/AP/HTPB propellant," *Journal of Thermal Analysis and Calorimetry*, vol. 143, no. 6, pp. 3935–3944, 2021.

[8] A. D. Baer and N. W. Ryan, "Ignition of composite propellants by low radiant fluxes," *AIAA Journal*, vol. 3, no. 5, pp. 884–889, 1965.

[9] C. E. Hermance, R. Shinnar, and M. Summerfield, "Ignition of an evaporating fuel in a hot, stagnant gas containing an oxidizer," *AIAA Journal*, vol. 3, no. 9, pp. 1584–1592, 1965.

[10] C. E. Hermance, "Implications concerning general ignition processes from the analysis of homogeneous, thermal explosions," *Combustion Science and Technology*, vol. 10, no. 5-6, pp. 261–265, 1975.

[11] T. Kashiwagi, "A radiative ignition model of a solid fuel," *Combustion Science and Technology*, vol. 8, no. 5-6, pp. 225–236, 1973.

[12] T. Niioka, M. Takahashi, and M. Izumikawa, "Ignition of double-base propellant in a hot stagnation-point flow," *Combustion and Flame*, vol. 35, no. 1, pp. 81–87, 1979.

[13] A. K. Kulkarni, M. Kumar, and K. K. Kuo, "Review of solid-propellant ignition studies," *AIAA Journal*, vol. 20, no. 2, pp. 243-244, 1982.

[14] Y. C. Liau, E. S. Kim, and V. Yang, "A comprehensive analysis of laser-induced ignition of RDX monopropellant," *Combustion and Flame*, vol. 126, no. 3, pp. 1680–1698, 2001.

[15] G. A. Risha, K. K. Kuo, D. E. Koch, and J. R. Harvel, "Laser ignition characterization of N-5 double-base solid propellants [J]," *International Journal of Energetic Materials and Chemical Propulsion*, vol. 5, no. 1-6, pp. 284–295, 2002.

[16] V. A. Arkhipov and A. G. Korotkikh, "The influence of aluminum powder dispersity on composite solid propellants ignitability by laser radiation," *Combustion and Flame*, vol. 159, no. 1, pp. 409–415, 2012.

[17] S. Jonathan and H. Yehuda, "Laser ignition of various pyrotechnic mixtures – an experimental study," *Propellants Explosives Pyrotechnics*, vol. 40, no. 5, pp. 755–758, 2015.

[18] V. Medvedev, V. Tsipilev, and E. Forat, "Effect of ammonium perchlorate and aluminum composition density on characteristics of laser ignition," *Propellants Explosives Pyrotechnics*, vol. 43, no. 2, pp. 122–125, 2018.

[19] V. Medvedev, V. Tsipilev, A. Reshetov, and A. Ilyin, "Conditions of millisecond laser ignition and thermostability for ammonium perchlorate/aluminum mixtures," *Propellants Explosives Pyrotechnics*, vol. 42, no. 3, pp. 243–246, 2017.

[20] J. Ehrhardt, L. Courty, P. Gillard, and B. Baschung, "Experimental study of pyrolysis and laser ignition of low-vulnerability propellants based on RDX," *Molecules*, vol. 25, no. 10, pp. 2276–2292, 2020.

[21] W. Pang, X. Fan, J. Yi et al., "Thermal behavior and non-isothermal decomposition reaction kinetics of NEPE propellant with ammonium dinitramide," *Chinese Journal of Chemistry*, vol. 28, no. 5, pp. 687–692, 2010.

[22] L. Kong, K. Dong, L. Pei, S. Chen, and C. Xia, "Study on mechanisms of AP decomposition and NEPE propellant oxygenizing and cross-linking," *Journal of Solid Rocket Technology*, vol. 43, no. 4, pp. 432–438, 2020.

[23] G. Q. Zhu, X. Chen, C. S. Zhou, and Q. J. Wu, "Study on laser ignition characteristics of NEPE propellant," *Advanced Materials Research*, vol. 549, no. 2, pp. 1037–1040, 2012.

[24] H. M. Wang, X. Chen, C. Zhao, G. Q. Zhu, and Q. H. Yang, "Study on ignition and combustion characteristics of NEPE propellant under laser irradiation," *Journal of Propulsion Technology*, vol. 36, no. 8, pp. 1262–1267, 2015.

[25] H. S. Xiang, X. Chen, C. S. Zhou, and H. J. Lai, "Effect of oxygen content in environment gas on the laser ignition process of NEPE propellant," *Chinese Journal of Explosives and Propellants*, vol. 39, no. 3, pp. 75–79, 2016.

[26] L. B. Li, X. Chen, C. S. Zhou, M. Zhu, and O. Musa, "Experimental investigation on laser ignition and combustion characteristics of NEPE propellant," *Propellants Explosives Pyrotechnics*, vol. 42, no. 9, pp. 1095–1103, 2017.

[27] C. Y. Tu, X. Chen, C. S. Zhou, B. C. Zhang, and L. B. Li, "Ignition and combustion characteristics of NEPE propellant in nitrogen and air," *Chinese Journal of Energetic Materials*, vol. 30, no. 8, pp. 811–818, 2022.

[28] C. Y. Tu, Y. Q. Zhuang, Y. K. Li et al., "Combustion process and aluminum agglomeration characteristics of NEPE propellant [J/OL]," *Journal of Aerospace Power*.

[29] C. Y. Tu, X. Chen, Y. K. Li, B. C. Zhang, and C. S. Zhou, "Experimental study of Al agglomeration on solid propellant burning surface and condensed combustion products," *Defence Technology*..

[30] C. Y. Tu, Z. G. Ling, L. L. Dong et al., "Dynamic behavior study of aluminum aggregates on the NEPE propellant combustion surface [J/OL]," *Journal of Propulsion Technology*https://kns.cnki.net/kcms/detail/11.1813.v.20220708.1250.002.html.

[31] A. Kakami, R. Hiyamizu, K. Shuzenji, and T. Tachibana, "Laser-assisted combustion of solid propellant at low pressures," *Journal of Propulsion and Power*, vol. 24, no. 6, pp. 1355–1360, 2008.

[32] L. Zheng, G. P. Pan, X. Chen, and L. Qiao, "Effect of magnesium powder particle size on combustion properties of Mg/PTFE fuel-rich propellant," *Chinese Journal of Energetic Materials*, vol. 18, no. 2, pp. 180–183, 2010.

[33] F. Q. Zhao, S. W. Li, and Y. Wang, "Study on the thermal decomposition of NEPE propellant (I) thermal decomposition of binder," *Journal of Propulsion Technology*, vol. 23, no. 3, pp. 249–251, 2002.

[34] Z. R. Liu, Z. H. Shi, and C. M. Yin, "Investigation on thermal decomposition of mixed systems of AP with RDX and HMX by DSC-TG-FTIR," *Chinese Journal of Explosives & Propellants*, vol. 30, no. 5, p. 57, 2007.

[35] J. C. Zhao, Q. J. Jiao, X. Y. Guo, Y. Guo, J. Y. Zhang, and Z. H. Wang, "Effect AP on the thermal stability of RDX and detonation performance of AP/RDX," *Chinese Journal of Explosive & Propellants*, vol. 42, no. 4, pp. 380–384, 2019.

[36] L. Mallick, S. Kumar, and A. Chowdhury, "Thermal decomposition of ammonium perchlorate–A TGA-FTIR-MS study: part I," *Thermochimica Acta*, vol. 610, pp. 57–68, 2015.

[37] M. B. Padwal and M. Varma, "Thermal decomposition and combustion characteristics of HTPB-coarse AP composite solid propellants catalyzed with Fe_2O_3," *Combustion Science and Technology*, vol. 190, no. 9, pp. 1–16, 2018.

[38] L. Liu, J. Li, L. Zhang, and S. Tian, "Effects of magnesium-based hydrogen storage materials on the thermal decomposition, burning rate, and explosive heat of ammonium perchlorate-based composite solid propellant," *Journal of Hazardous Materials*, vol. 342, pp. 477–481, 2018.

[39] A. N. Ali, S. F. Son, B. W. Asay, M. E. Decroix, and M. Q. Brewster, "High-irradiance laser ignition of explosives," *Combustion Science and Technology*, vol. 175, no. 8, pp. 1551–1571, 2003.

[40] L. Ping, B. J. Nan, P. Wu, and X. M. Ma, "Study on laser ignition characteristics of a high energy propellant," *Journal of Gun Launch and Control*, vol. 15, no. 2, pp. 28–31, 2009.

[41] T. Kashiwagi, B. W. Macdonald, H. Isoda, and H. Summerfield, "Ignition of a solid polymeric fuel in a hot oxidizing gas stream," *Symposium on Combustion*, vol. 13, no. 1, pp. 1073–1086, 1971.

[42] A. N. Ali, M. M. Sandstrom, D. M. Oschwald, K. M. Moore, and S. F. Son, "Laser ignition of DAAF, DHT and DAATO (3.5)," *Propellants Explosives Pyrotechnics*, vol. 30, no. 5, pp. 351–355, 2005.

[43] M. Zarzecki, J. G. Quintiere, R. E. Lyon, T. Rossmann, and F. J. Diez, "The effect of pressure and oxygen concentration on the combustion of PMMA," *Combustion and Flame*, vol. 160, no. 8, pp. 1519–1530, 2013.

[44] W. Zhang, H. Zhu, D. Y. Fang, Z. X. Xia, and J. G. Xue, "Research on test method of combustion performance of lean oxygen propellant at low pressure," *Chinese Journal of Energetic Materials*, vol. 7, no. 3, pp. 118–121, 1999.

[45] A. P. Denisyuk, Y. G. Shepelev, D. L. Rusin, and I. V. Shumskii, "Effect of RDX and HMX on the efficiency of catalysts for double-base propellant combustion," *Combustion, Explosion, and Shock Waves*, vol. 37, no. 2, pp. 190–196, 2001.

[46] V. P. Sinditskii, V. Y. Egorshev, V. V. Serushkin, S. A. Filatov, and A. N. Chernyi, "Combustion mechanism of energetic binders with nitramines," *International Journal of Energetic Materials & Chemical Propulsion*, vol. 11, no. 5, pp. 427–449, 2012.

[47] A. P. Denisyuk, Z. N. Aung, and Y. G. Shepelev, "Energetic materials combustion catalysis: necessary conditions for implementation," *Propellants Explosives Pyrotechnics*, vol. 46, no. 1, pp. 90–98, 2021.